

Ultrafast Proton Transfer Reaction in Phenol-(Ammonia)_n Clusters: An *Ab-Initio* Molecular Dynamics Investigation

Reman Kumar Singh[†] (orcid.org/0000-0001-6160-4586)

Rakesh Pant[†] (orcid.org/0000-0001-7781-5812)

G. Naresh Patwari* (orcid.org/0000-0003-0811-7249)

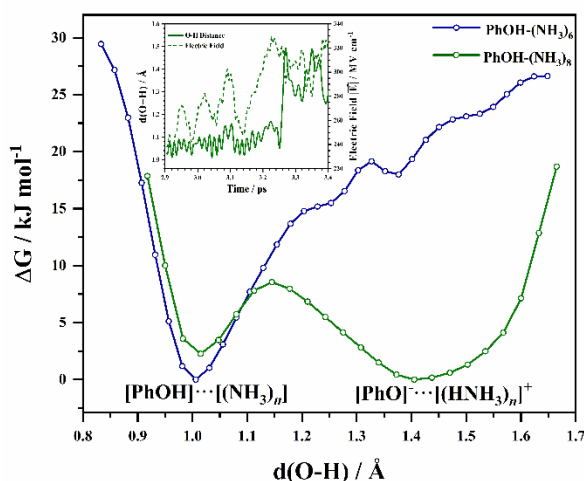
Department of Chemistry, Indian Institute of Technology Bombay, Powai, Mumbai
400076 INDIA.

[†] These authors have contributed equally

* Email: naresh@chem.iitb.ac.in

ABSTRACT

The ability of phenol to transfer the proton to surrounding ammonia molecules in a phenol-(ammonia)_n cluster will depend on the relative orientation of the ammonia molecules and a critical field of about 285 MV cm⁻¹ is essential along the O-H bond for the transfer process. *Ab-initio* MD simulations reveal that for a spontaneous proton transfer process, the phenol molecule must be embedded in a cluster consisting of at least eight ammonia molecules, even though several local minima with proton transferred can be observed for clusters consisting of 5-7 ammonia molecules. Further, phenol solvated in large clusters of ammonia, the proton transfer is spontaneous with the proton transfer event being instantaneous (about 20-120 fs). These simulations indicate that the rate-determining step for the proton transfer process is the reorganization of the solvent around the OH group and the proton transfer process in phenol-(ammonia)_n clusters. The fluctuations in the solvent occur until a particular set of configurations projects the field in excess of critical electric field along the O-H bond which drives the proton transfer process with a response time of about 70 fs. Further, the proton transfer process follows a curvilinear path which includes the O-H bond elongation and out-of-plane movement of the proton and can be referred to as a “Bend-to-Break” process.



INTRODUCTION

The role of solvent in the proton transfer process is paramount and determines whether or not the proton transfer will occur and the physicochemical properties of the solvent determines the pK_a of the solute and illustrated by the fact pK_a of HCl in water (-7.0) and acetonitrile (10.3) differ by more than 17 units.¹ These differences in the pK_a can be related to the free-energy proton extraction by the solvent and solvation free energy of the proton and the counter anion. One of the interesting aspects of the free-energy proton extraction by the solvent is the role of microscopic solvation of the solute centred around the protic group. More importantly, the general interest is to probe the minimum number of solvent molecules required for acid dissociation and concurrent proton transfer process, to understand the acid dissociation phenomenon at a molecular level.²⁻⁶ In this regard, the role of ammonia as a solvent in the proton transfer process in the phenol-(ammonia)_n clusters have been the subject of intense experimental and theoretical investigations by several research groups over the past three decades to understand the proton transfer reaction in the ground state and hydrogen transfer process in the excited electronic state.⁷⁻¹⁶ Additionally, it has been shown that the excited proton transfer reaction of phenol becomes ultrafast at the air-water interface.¹⁷

The proton transfer reaction of phenol-(ammonia)_n clusters were investigated using the infrared spectroscopic method, which revealed that at least six ammonia molecules are required to observe the features corresponding to the proton transferred form in the ground state.¹⁴ On the other hand, electronic structure calculations have shown that five ammonia molecules are adequate to extract the proton from phenol, in the ground state, albeit being energetically unfavourable, and the proton transfer process in the phenol-(ammonia)_n clusters becomes increasingly favourable with the increase in the number of ammonia molecules and become spontaneous with nine or more number of ammonia molecules.¹⁶ On the contrary, in the case of or the [PhOH-(NH₃)₂₋₆]⁺ cluster cations, proton transfer is spontaneous even in the presence of two ammonia molecules.¹⁸ In a recent work our group, with the aid of electric field calculations along the donor O-H of phenol in the phenol-(ammonia)_n clusters, using at the M06-2X/cc-pVTZ level of theory, has shown that a critical field of 236 MV cm⁻¹ is essential to transfer of a proton from phenol to the surrounding ammonia cluster.¹⁹ Interesting, six

exceptions to this rule were observed, which indicates that the projection of the solvent electric field over the O–H bond is not an unqualified descriptor of the proton transfer reaction. Based on these observations, it was noted that the critical electric field is a necessary, but not sufficient condition for the proton transfer process. However, the usage of DFT methodologies can lead to artefacts in calculating the molecular electrostatic potentials for the proton transfer process, consequently misrepresenting the value of the critical electric field.²⁰ Furthermore, the unique feature of the proton transfer process in the phenol-(ammonia)_n clusters is the out-of-plane motion of the proton concurrent with the O–H bond elongation leading to a curvilinear path, which has been referred to as a “Bend-to-Break” process.¹⁹ However, the curvilinear path for the proton transfer process was assessed based on the snapshots that were optimized using electronic structure calculations. In this work, the proton transfer process in the phenol-(ammonia)_n clusters, in the ground state, is re-evaluated using electric field calculations at the MP2 level theory and Born-Oppenheimer molecular dynamic (BOMD) simulations were carried out to understand the trajectory of the proton motion.

METHODOLOGY

The geometries of 126 PhOH-(NH₃)_n (n=1-10) clusters, calculated using M06-2X/cc-pVTZ method, were reported earlier,¹⁶ and among these 126 structures only 114 structures which show hydrogen bonding between the phenolic OH group to the surrounding ammonia cluster and were considered.¹⁹ These 114 structures were re-optimized using the resolution of identity second-order perturbation theory (RI-MP2) method with cc-pVDZ basis set using ORCA 4.1.2 suite of programs.²¹ Following, the electric field along the O–H bond was calculated on the 114 structures using the procedure described elsewhere.^{19,22-26} The nomenclature used to label the structures is identical to that reported by Shimizu et al.,¹⁶ wherein each structure is labelled by an alphanumeric. For instance, the label 7A indicates the most stable phenol-(ammonia)₇ complex, while the label 5C indicates the third most stable phenol-(ammonia)₅ complex. Further, BOMD simulations were carried out for several phenol-(ammonia)_n clusters were carried out using twenty (20) selected starting geometries reported earlier,¹⁶ viz. 1A, 2A, 3A, 4A, 4B,

5A, 5C, 6A, 6B, 6E, 7A, 7B, 7C, 8A, 8B, 8C, 9B, 10C, 10E and 10F (see the SI for the coordinates). BOMD calculations were carried out using long-range dispersion corrected density functional BLYP-D3/def2-SVP with a time step of 0.5 fs. The simulation temperature was fixed at 10 K, since the gas-phase experiments are carried out using molecular beams with low internal temperatures and 10 K would be a good comparison.^{7,14} All the calculations were carried out using ORCA 4.1.2 suite of programs.²¹ The length of the BOMD trajectories was up to 35 ps in some cases to sample the probability of the proton transfer process. The choice of DFT method for the BOMD simulations is due the fact that the DFT method is reasonable for obtaining the geometry, however, has shortcomings in calculating the molecular electrostatic potentials.²⁰

Alternately, initial configurations for BOMD simulations were extracted from the classical MD simulations for PhOH-(NH₃)_n (n=1-8) clusters. For the clusters with n ≥ 3, the initial configuration for the BOMD simulations consists of phenol moiety in the single donor and double acceptor (DAA) motif. Additionally, MD simulations on a PhOH embedded in ammonia molecules with a 3.4 nm cubic box was carried out and the lowest energy configuration from MD trajectory was taken and truncated the solvation shell after 8 Å from the centre of mass of phenol, yielding a PhOH-(NH₃)₆₃ cluster, which was further considered for BOMD simulations. For all these clusters, unrestrained simulation using NVT ensemble were carried out for 30 ps. The temperature was fixed at 150 K using the canonical sampling velocity rescale (CSVR) method with a coupling constant of 1 fs. In small clusters the enthalpic and entropically oppose each other leading to formation of the cluster assembly and consequent proton transfer, in the present scenario 150 K was found to be a good compromise, *vide infra*. The BOMD simulations, in this case, were carried out using long-range dispersion corrected BLYP density functional (BLYP-D3) in combination with dzVP basis set. The temperature equilibrated within 1 ps of simulation time and fluctuate around 150 K throughout the trajectories of about 30 ps (Figure S1, see the SI). Thereafter, well-tempered metadynamics simulations were carried out for PhOH-(NH₃)_n clusters consisting of up to seven ammonia molecules by biasing the O-H bond distance with a Gaussian potential of 3 kcal mol⁻¹ height and 0.05Å width. Thereafter potentials of mean force along the O-H bond distance were constructed. The BOMD simulations were carried out using CP2K-6.2 package.²⁷

RESULTS AND DISCUSSION

(A) Role of electric field

In the case of $\text{PhOH}-(\text{NH}_3)_9$ clusters two structures within an energy difference of 0.8 kJ mol^{-1} show different behaviour relative to their ability to transfer the proton as can be seen in Figure 1 (these two correspond to structures 9A and 9B in Ref.16). Thus, the ability of the ammonia cluster surrounding the phenol molecule to extract the proton depends on the distribution of the ammonia molecules and not the stabilization energy. The reoptimization of the M06-2X/cc-pVTZ structures using RI-MP2/cc-pVDZ level reveals that, in general, the gross structure of the cluster remains unaltered with few exceptions, wherein four structures (5K, 8S, 6G, 6L and 8S) which did not result in proton transfer at the M06-2X/cc-pVTZ level exhibit proton transfer at RI-MP2 level of theory. In the case of $\text{HCl}-(\text{DMSO})_n$ clusters, it was shown that the electric field calculations using MP2 method were comparable for the structures optimized using MP2 and DFT methods.²⁰ Therefore, the proton transfer process from phenol to ammonia is examined in terms of the electric field calculated at the RI-MP2/cc-pVDZ level along the O–H bond for the structures optimized using RI-MP2/cc-pVDZ (red data points in Figure 1C) and M06-2X/cc-pVTZ (blue data points in Figure 1C) methods and the resulting plot of the O–H distances against the corresponding electric fields is shown in Figure 1. The critical electric fields obtained for the RI-MP2/cc-pVDZ//RI-MP2/cc-pVDZ and RI-MP2/cc-pVDZ//M06-2X/cc-pVTZ methods are 285.2 and 292.7 MV cm^{-1} , respectively. In comparison, the electric field calculated M06-2X/cc-pVTZ level shows much lower critical electric field value of 236.2 MV cm^{-1} along the O–H bond.¹⁹ Moreover, the M06-2X/cc-pVTZ level calculation also showed six exceptions (Figure S2, see the SI), wherein the proton transfer from phenol to ammonia was not observed even though the electric field along the O–H bond value exceeded the critical electric field value.¹⁹ On the contrary, the electric field calculations using RI-MP2/cc-pVDZ level for both RI-MP2/cc-pVDZ and M06-2X/cc-pVTZ optimized structures, the proton transfer is observed if the electric field along the O–H bond exceeds the critical electric field, without exceptions. The present set of results along with those of $\text{HCl}-(\text{DMSO})_n$ clusters,²⁰ illustrate that the observed differences in estimating the critical electric fields using MP2 and DFT (M06-2X functional in the present case) methods does not originate from the structural factors of the cluster, but due to errors in calculating the molecular electrostatic potentials (MESP) using DFT

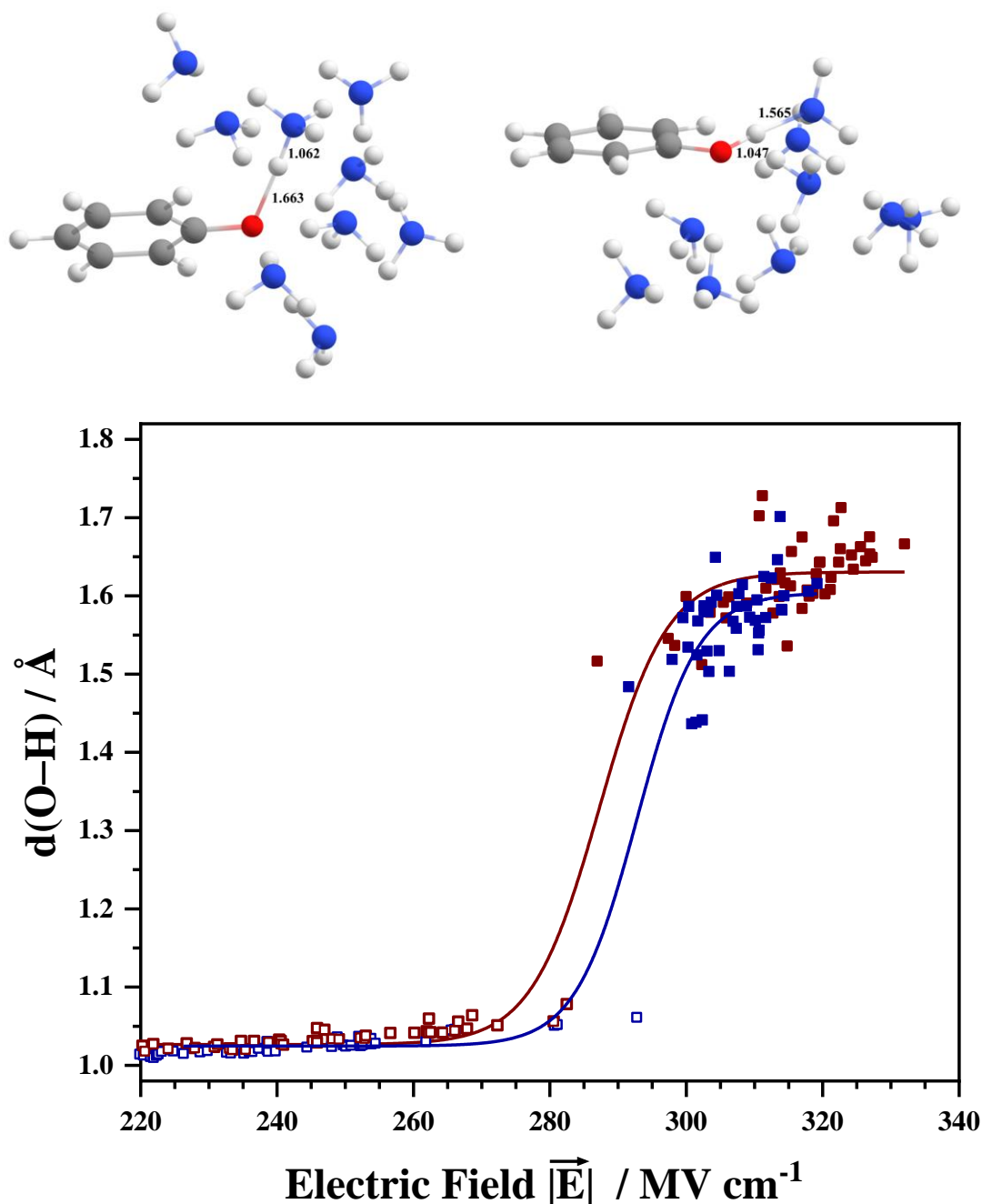


Figure 1. (Top) Two representative structures of PhOH-(NH₃)₉ (9A; left and 9B; right) with the stabilization energy difference of 0.8 kJ mol⁻¹, which illustrates the difference in the ability of proton transfer from phenol to ammonia cluster depends on the orientation of the ammonia molecules. Notice the difference in the distribution of the ammonia molecules around phenol in the two structures. (Bottom) The plots of O-H distance in PhOH-(NH₃)_n clusters against the corresponding electric fields. The red and blue data points correspond to structures optimized using RI-MP2/cc-pVDZ and M06-2X/cc-pVTZ methods while the electric field is calculated at RI-MP2/cc-pVDZ level in both the cases. The solid lines are the nonlinear Boltzmann sigmoidal fit to the calculated data points around the point of inflection. The points of inflection correspond to electric field values of 285.2 and 292.7 MV cm⁻¹ for the structures optimized at RI-MP2/cc-pVDZ and M06-2X/cc-pVTZ methods, respectively. See the SI for the coordinates of 9A and 9B structures.

methods. Thus, the limitations of DFT theory to appropriately model the proton transfer reactions in terms of accurate description MESP can be attributed to the importance of HF exchange,²⁸ which is generally under-represented in the exchange-correlation functionals due to energy fitting function with having small (about 0.2) coefficient for the exchange energy.²⁹

(B) Proton transfer in BOMD simulations

Several reports in the literature deal with the question of the minimum number of ammonia molecules required in a cluster around phenol for the spontaneous proton transfer, and the consensus is that eight ammonia molecules are required for spontaneous proton transfer from the phenol to ammonia cluster. However, the assessment of the proton transfer process using electric fields indicates that a critical electric solvent electric field along the O–H bond is a necessary requirement for the proton transfer, which depends on the solvent configuration. Electronic structure calculations reveal that some of the $\text{PhOH}-(\text{NH}_3)_n$ clusters show proton transfer with 5-7 molecules of ammonia, however, these structures are higher in energy relative to the global minimum.¹⁶ In order to access the proton transfer dynamics in $\text{PhOH}-(\text{NH}_3)_n$ clusters, BOMD simulations starting from selected $\text{PhOH}-(\text{NH}_3)_{1-4}$ clusters (structures 1A, 2A, 3A, 4A, 4B geometries, see the SI for coordinates) were carried out, and the corresponding trajectories reveal that the proton transfer does not occur in the simulation time of 30 ps, even though in this case (for 4B) the O–H bond elongates to 1.10 Å. Further, the BOMD trajectories were also calculated for several $\text{PhOH}-(\text{NH}_3)_{5-10}$ clusters (starting from 5A, 5C, 6A, 6B, 6E, 7A, 7B, 7C, 8A, 8B, 8C, 9B, 10C, 10E, and 10F geometries, from Ref. 16). Among these, eight trajectories (starting from 5A, 5C, 6E, 7A, 9B, 10C, and 10E) resulted in the proton transfer process, whereas, simulations starting from 6A, 6B, 7A, 7C, 8A, 8B, 8C, and 10F geometries did not yield proton transfer even after 35 ps simulation time. However, the (simulation) time required of the proton transfer varied due to differences in the initial structure and the structural landscape sampled during the simulation. The plot of O–H distance in the BOMD trajectory It can be noticed from Figure 2 that the actual proton transfer process occurs almost instantaneously (about 120 fs) between the time-points 5A-2 to 5A-4 and 9B-2 to 9B-4, following solvent reorganization. Table S1 (see the SI) summarizes the proton transfer time and the corresponding C-C-O-H dihedral angle (χ), which captures the out-of-plane movement of the OH proton. For the eight trajectories in which the

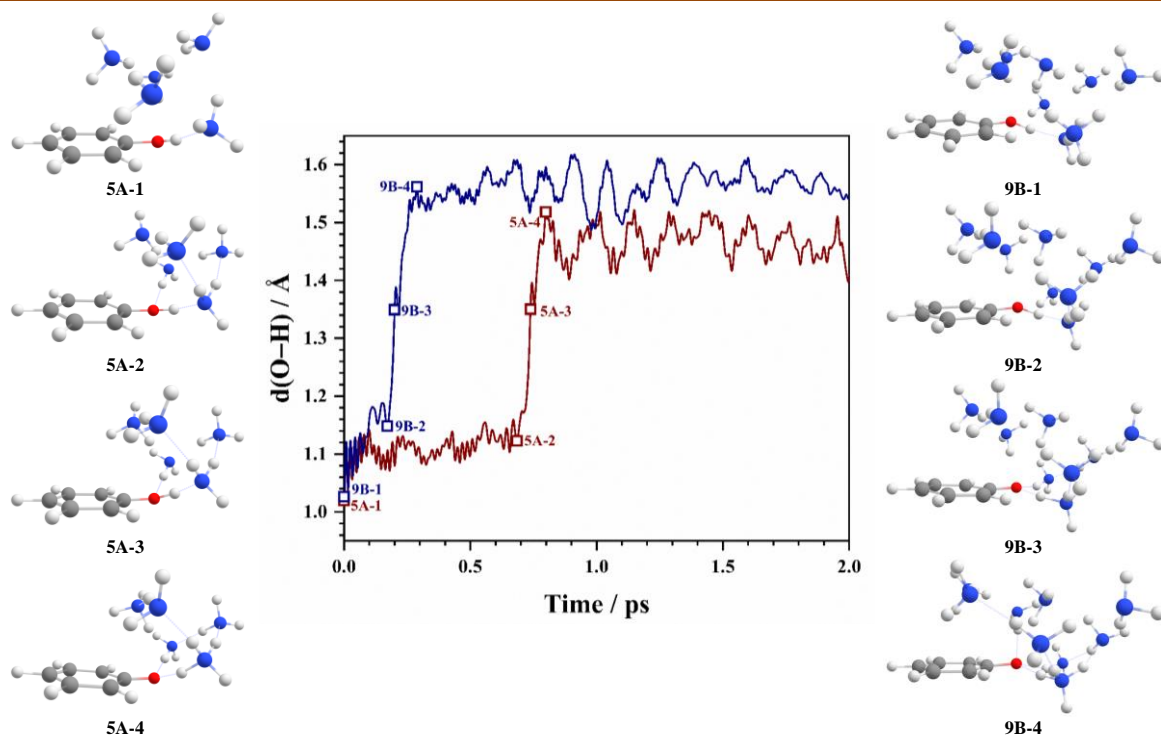


Figure 2. (Middle) The plot of O–H distance as a function of simulation time for the two BOMD trajectories starting from the initial structures 5A (red-trace) and 9B (blue trace). In both the cases, proton transfer from the phenol moiety to the ammonia cluster was observed which is indicated by the lengthening of the OH bond. (Left and Right panels) Set of structures along the BOMD trajectories for $\text{PhOH}-(\text{NH}_3)_5$ and $\text{PhOH}-(\text{NH}_3)_9$ clusters starting initial configuration of 5A and 9B as they evolve along the proton transfer trajectory. The time points corresponding to the structures shown are marked on the corresponding trajectories. Notice that the time taken for the proton transfer in the two cases is different and is indicative of the fact that different trajectories sample different parts of the structural landscape. It can also be noticed in both the trajectories, the actual proton transfer process (the sigmoidal part of the curve) occurs almost instantaneously (about 120 fs) from the time-points 5A-2 to 5A-4 and 9B-2 to 9B-4, following solvent reorganization. See the SI for the coordinates of the various snapshots shown in this figure.

proton transfer happens, the dihedral angle χ varies from 0.6° to 42.0° with an average of 15° , suggesting a curvilinear proton transfer from the phenol to ammonia cluster. These results are in agreement with an earlier work in which it was shown that the proton transfer from the phenol moiety to the surrounding ammonia cluster is accompanied by the out-of-plane motion of the OH proton.¹⁹ It must however be noted that the possibility of proton transfer process along these trajectories will depend on the geometries sampled, therefore do not yield thermodynamic parameters.

(C) Potentials of mean force for the proton transfer reaction

Alternatively, potentials of mean force for the $\text{PhOH}-(\text{NH}_3)_{1-8}$ clusters were constructed, which are depicted in Figure 3. For $\text{PhOH}-(\text{NH}_3)_{1-8}$ clusters the free energy for the proton transferred species $[\text{PhO}]^- [\text{H}(\text{NH}_3)_n]^+$ decreases gradually with the increase in the number of ammonia molecules and becomes spontaneous for a cluster consisting of eight ammonia molecules, even though electronic structure calculations suggest that the proton transfer process becomes spontaneous for $n \geq 9$.¹⁶ As shown earlier using BOMD simulations, the proton transfer from the phenol moiety can be observed for clusters consisting of $5 \leq n \leq 7$, however, in these cases the proton transferred structures correspond to local minima on the free energy surface and do not truly represent the spontaneity of the proton transfer process. Additionally, in the BOMD trajectories with $n \leq 7$ back proton transfer was observed, the probability of which decreases with the number of ammonia molecules in the cluster (Figure S3, see the SI), which can be attributed to the spontaneity (or lack of it) in smaller clusters. In the case of small clusters ($n \leq 8$) the number of ammonia molecules are too few to form second solvation shell. In this case the phenolate and the ammonium ions exist as contact ion pair. However, in a small fraction (about 4%) of these contact ion pairs the ammonium ion is rotated in such a way that the transferred proton moves away from the oxygen atom of the phenolate ion. On the other hand, in the case of $\text{PhOH}-(\text{NH}_3)_{63}$ cluster, the diffusion of the ammonium ion to second solvation shell was observed.

The potentials of mean force for the $\text{PhOH}-(\text{NH}_3)_8$ cluster were calculated by varying the temperature in the range 100 to 300 K, however, proton transfer not observed beyond 200 K, therefore the data above 200 K is neglected. Figure 3 shows the plots of ΔG (relative to undissociated form) as a function of O–H bond distance for 100 to 200 K temperatures. The corresponding plot of ΔG for the proton transferred structure as a function of temperature is also shown in Figure 3. Based on these results it can be inferred that proton transfer occurs only in a limited temperature range of about 120-160 K, with 150 K being the optimum temperature. The spontaneous proton transfer in the $\text{PhOH}-(\text{NH}_3)_8$ cluster in the small range of temperatures can be attributed to the competition between the enthalpic and entropic contributions of the formation of the cluster and the proton transfer process.

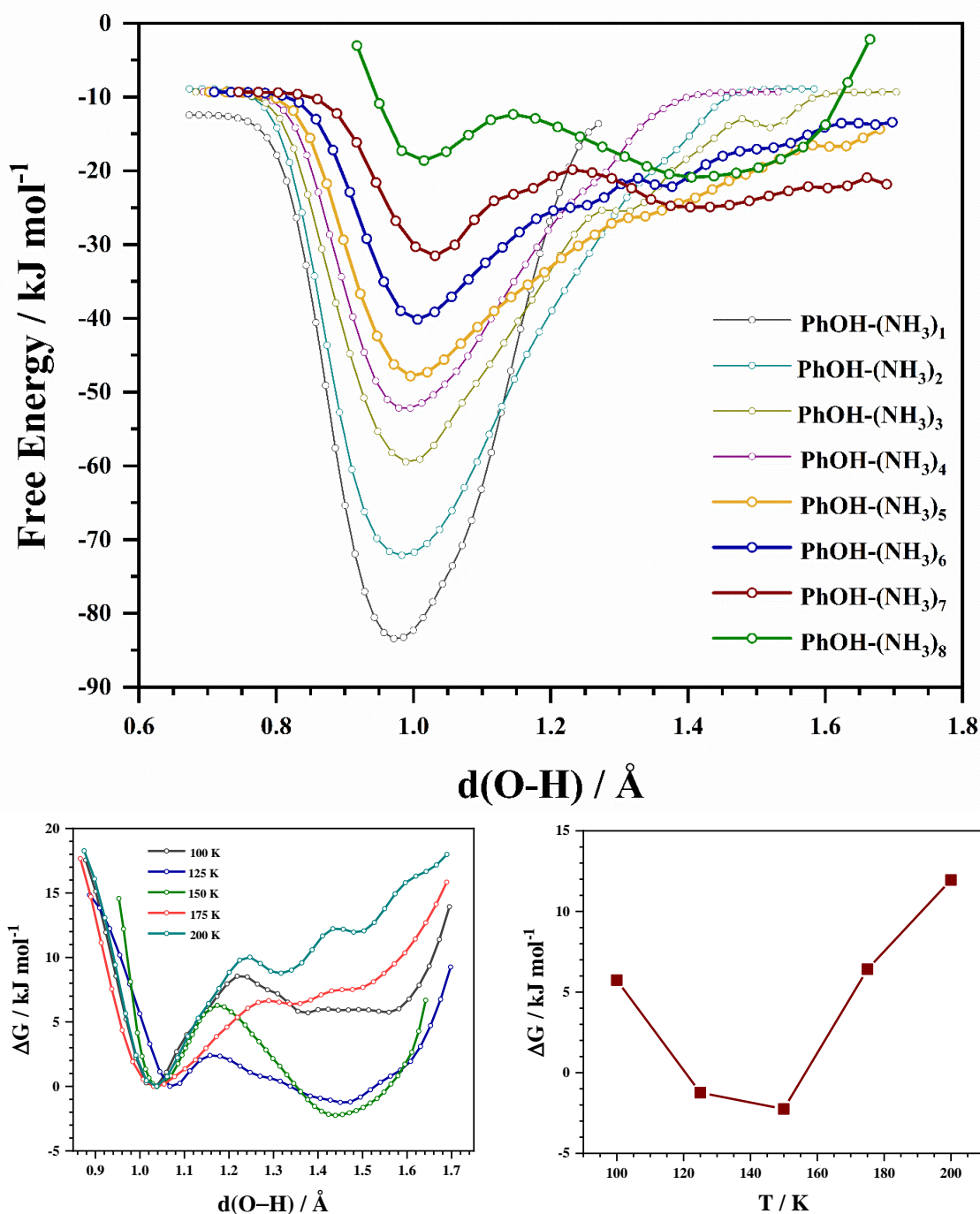


Figure 3. (Top) Potentials of mean force as a function of phenolic O-H distance obtained from metadynamics simulations by biasing the O-H bond distance with a Gaussian potential of 3 kcal mol⁻¹ height and 0.05 Å width for PhOH-(NH₃)₁₋₇ clusters. In the case of PhOH-(NH₃)₈ cluster, the proton transfer was spontaneous, therefore biasing potential along the O-H bond was not required. (Bottom-Left) Plot of the ΔG (relative to the undissociated form of the PhOH-(NH₃)₈ cluster) as a function of O-H bond distance for various temperatures ranging from 100–200 K. (Bottom-Right) Plot of the maximum change in ΔG for the proton transferred structure relative to the undissociated form as a function of temperature. The proton transferred from has lowest ΔG at 150 K, which indicates that the probability of proton transfer is maximum at this temperature.

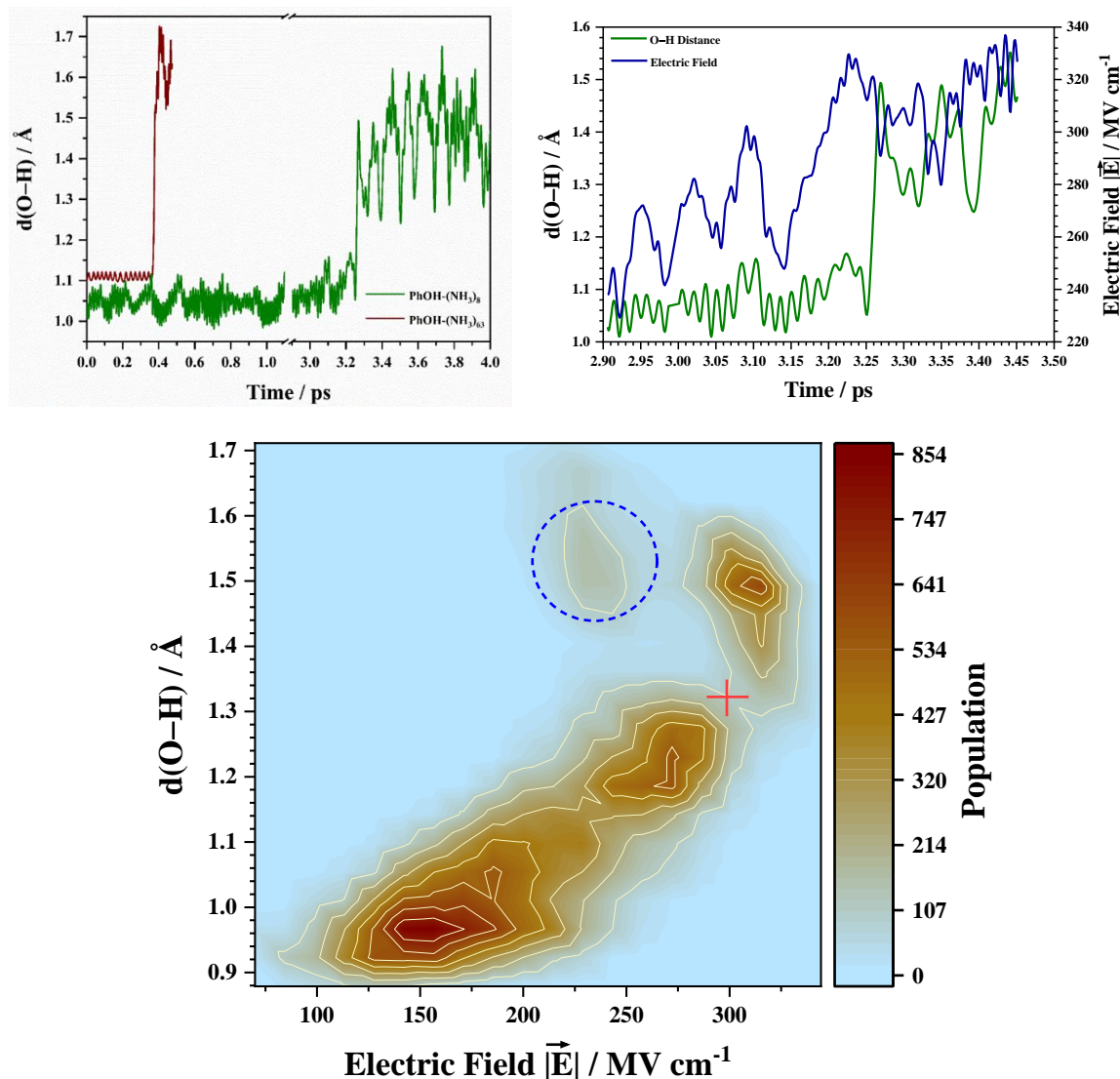


Figure 4. (Top-left) The plot of O-H distance as a function of simulation time for the two BOMD trajectories at 150 K for the $\text{PhOH}-(\text{NH}_3)_8$ (green curve) and $\text{PhOH}-(\text{NH}_3)_{63}$ (red curve) clusters, wherein spontaneous proton transfer was observed. The initial part of the trajectory indicates the solvent reorganization followed by instantaneous proton transfer within the time scale of about 20 fs. (Top-right) The plots of O-H distance (green curve) and electric field (blue curve) as a function of simulation time for the $\text{PhOH}-(\text{NH}_3)_8$ cluster in the time window of proton transfer. Notice the response of the proton transfer to the change in electric field in the time window of 3.15 to 3.30 ps. The green curves in the both top panel plots are from the same trajectory. (Bottom) Surface plot showing the population distribution of O-H distances as a function of electric field along the O-H bond. The electric field was calculated for 38149 snapshots of $\text{PhOH}-(\text{NH}_3)_{4-8}$ clusters generated in the BOMD trajectories using RI-MP2/cc-pVDZ level. The O-H distance (0.87-1.73 \AA) and the electric field (70-340 MV cm^{-1}) was divided into 25 equally spaced bins. The cross-sign indicates that an electric field of 298.7 MV cm^{-1} is required for the proton transfer process, which is marginally more than the critical electric field of 292.7 MV cm^{-1} , for the DFT optimized structures. The data in the circled region represents a small fraction (about 4%) of proton transferred structures wherein the ammonium ion rotates away from the phenolate ion.

The OH distance along the BOMD trajectory for the $\text{PhOH}-(\text{NH}_3)_8$ and $\text{PhOH}-(\text{NH}_3)_{63}$ clusters at 150 K, shown in Figure 4, signifies the time for the solvent reorganization around the phenolic OH group is the rate-determining step of the proton transfer process and the proton transfer event is almost instantaneous (about 20 fs). Incidentally, the proton transfer event for the two trajectories shown in Figure 2 is about 120 fs. Therefore, based on the BOMD simulations, it be concluded that the rate-determining step for the proton transfer process is the reorganization of the solvent around the OH group. The electric field along the O–H bond for the $\text{PhOH}-(\text{NH}_3)_8$ cluster as a function of simulation time in the time window of proton transfer (about 2.9-3.5 ps) is also depicted in Figure 4. The electric field along the trajectory starts increasing around 3.15 ps and sustains over the critical electric field value of about 290 MV cm^{-1} for over 60 fs and the proton transfer follows with a response time (delay of) about 70 fs. These results suggest that ~~when~~ the solvent electric field drives the proton transfer process. Therefore, fluctuations in solvent configuration occur until a particular set of configurations projects the field in excess of critical electric field along the O–H bond, resulting in the proton transfer on a relatively faster time scale (within 20fs). Further, the electric field was calculated over the all the BOMD 38149 snapshots for the $\text{PhOH}-(\text{NH}_3)_{4-8}$ clusters and the resulting surface plot showing the population of O–H distances as a function of electric field along the O–H bond is shown in Figure 4. The surface plot indicates that an electric field of 298.7 MV cm^{-1} is required for the proton transfer process, which is marginally more than the critical electric field of 292.7 MV cm^{-1} for the DFT optimized structures. Moreover, the surface plot also shows presence of a small fraction (about 4%) of proton transferred structures wherein the ammonium ion rotates away from the phenolate ion (encircled region).

One of the important attributes of the proton transfer process in the $\text{PhOH}-(\text{NH}_3)_n$ clusters is the out-of-plane motion of the OH proton during the proton transfer process, as indicated by the C–C–O–H dihedral angle (χ). Figure 5 depicts that normalized distribution plot of the angle χ for proton transferred species in the O – H distance interval 1.30-1.65 Å, obtained from the BOMD trajectories of $\text{PhOH}-(\text{NH}_3)_{2-8}$ clusters, which shows a maximum around 25° and a weighted average of 17° . Alternatively, a surface plot showing the population distribution of angle χ as a function of O–H distance for all the snapshots obtained from the BOMD trajectories of $\text{PhOH}-(\text{NH}_3)_{2-8}$ clusters is shown in Figure S4 (see the SI) and the subset for the proton transferred structures is shown

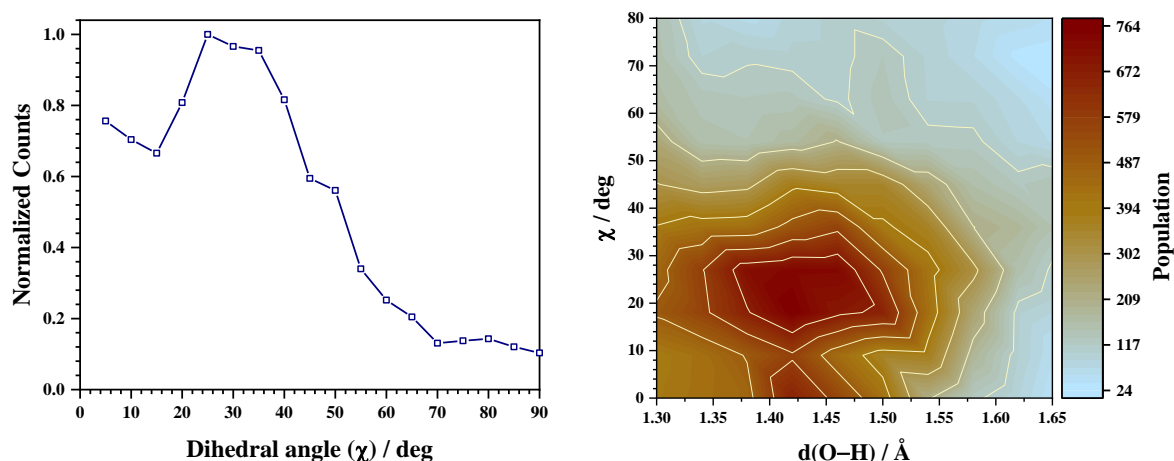


Figure 5. (Left) Normalized distribution plot of out-of-plane dihedral angle (χ) (bin size of 5°) for the proton transferred structures in the BOMD trajectories of PhOH-(NH₃)₂₋₈ clusters. (B) Surface plot showing the population distribution of out-of-plane dihedral angle (χ) as a function of O-H distance for the proton transferred structures in the BOMD trajectories of PhOH-(NH₃)₂₋₈ clusters. In the maximum probability is around 25° in both the plots.

in Figure 5, which once again shows maximum probability around 25°. However, the data for the undissociated clusters (Figure S4, see the SI) shows a large spread in the angle χ , which indicates that the OH bond is predisposed for the out-of-plane motion of the OH group during the proton transfer process. These results are in agreement with an earlier work in which it was shown that the proton transfer from the phenol moiety to the surrounding ammonia cluster is accompanied by the out-of-plane motion of the OH proton, leading to a “Bend-to-Break” process.¹⁹ The out-of-plane motion of the OH can be rationalized on the fact that the proton transformed form corresponds formation of phenolate and ammonium ions. The interaction of the ammonium ion with the phenolate ion resembles the benzene-ammonium cation- π complex.³⁰ The proton transfer path from phenol to ammonia connects these two end points, in which the OH group will move away from the plane of the phenyl ring as the reaction progresses and can be classified as “Bend-to-Break” process.

CONCLUSIONS

The proton transfer reaction in the phenol-(ammonia)_n clusters was investigated using electronic structure calculations using RI-MP2/cc-pVDZ level of theory in

combination with *Ab-Initio* (Born-Oppenheimer) MD simulations. The electric field calculations indicate that a critical electric field of about 285 MV cm⁻¹ is required along the O–H bond for the transfer of proton transfer process. Further, the BOMD simulations reveal that the proton transfer does not occur in phenol-(ammonia)_n clusters with $n \leq 4$, while for $n \leq 5-7$, several local minima can be found wherein the proton transfer can occur and finally for clusters with $n \geq 8$ proton transfer is spontaneous. In the case of large clusters and extending the analogy to phenol solvated in ammonia, the proton transfer is instantaneous and spontaneous. The *Ab-Initio* MD simulations suggest that the solvent reorganization around the phenol OH group is the rate-determining step for the proton transfer process. The electric field along the OH group acts as a trigger for the proton transfer to occur. Further, both the electronic structure and BOMD simulations suggest that the proton transfer process in the phenol-(ammonia)_n clusters follows a curvilinear involving the elongation of the O–H bond and the out-of-plane motion of the OH proton.

ACKNOWLEDGEMENTS

RKS and RP thank IIT Bombay for the Institute Postdoctoral Fellowship. Authors gratefully acknowledge SpaceTime-2 supercomputing facility at IIT Bombay for the computing time. The support and the resources provided by 'PARAM Brahma Facility' under the National Supercomputing Mission, Government of India at the Indian Institute of Science Education and Research (IISER) Pune are gratefully acknowledged. Authors also gratefully acknowledge the SpaceTime-2 supercomputing facility at IIT Bombay for the computing time.

SUPPORTING INFORMATION

The Supporting Information is available.

Plots showing temperature fluctuation for the BOMD simulations, plots showing electric field along the OH bond calculated using M06-2X/cc-pVTZ level, plots of O–H distance as a function of simulation time for the PhOH-(NH₃)₄₋₈ clusters, surface plot of population

depicting out-of-plane motion of the OH group, table containing proton transfer data, OH distances and CCOH dihedral angle (χ) and geometries of selected structures (PDF).

REFERENCES

- (1) Kütt, A.; Rodima, T.; Saame, J.; Raamat, E.; Mäemets, V.; Kaljurand, I.; Koppel, I. A.; Garlyauskayte, R. Y.; Yagupolskii, Y. L.; Yagupolskii, L. M.; Bernhardt, E.; Willner, H.; Leito, I. Equilibrium Acidities of Superacids. *J. Org. Chem.* **2011**, *76*, 391–395.
- (2) Pérez De Tudela, R.; Marx, D. Acid Dissociation in HCl-Water Clusters Is Temperature Dependent and Cannot Be Detected Based on Dipole Moments. *Phys. Rev. Lett.* **2017**, *119*, 223001.
- (3) Gutberlet, A.; Schwaab, G.; Birer, Ö.; Masia, M.; Kaczmarek, A.; Forbert, H.; Havenith, M.; Marx, D. Aggregation-Induced Dissociation of HCl(H₂O)₄ Below 1 K: The Smallest Droplet of Acid. *Science* **2009**, *324*, 1545–1549.
- (4) Weimann, M.; Fárnik, M.; Suhm, M. A. A First Glimpse at the Acidic Proton Vibrations in HCl-Water Clusters via Supersonic Jet FTIR Spectroscopy. *Phys. Chem. Chem. Phys.* **2002**, *4*, 3933–3937.
- (5) Flynn, S. D.; Skvortsov, D.; Morrison, A. M.; Liang, T.; Choi, M. Y.; Douberly, G. E.; Vilesov, A. F. Infrared Spectra of HCl-H₂O Clusters in Helium Nanodroplets. *J. Phys. Chem. Lett.* **2010**, *1*, 2233–2238.
- (6) Maity, D. K. How Much Water Is Needed to Ionize Formic Acid? *J. Phys. Chem. A* **2013**, *117*, 8660–8670.
- (7) Iwasaki, A.; Fujii, A.; Watanabe, T.; Ebata, T.; Mikami, N. Infrared Spectroscopy of Hydrogen-Bonded Phenol - Amine Clusters in Supersonic Jets. *J. Phys. Chem.* **1996**, *100*, 16053–16057.
- (8) Steadman, J.; Syage, J. A. Picosecond Studies of Proton Transfer in Clusters. 2. Dynamics and Energetics of Solvated Phenol Cation. *J. Am. Chem. Soc.* **1991**, *113*, 6786–6795.
- (9) Syage, J. A. Tunneling Mechanism for Excited-State Proton Transfer in Phenol-Ammonia Clusters. *J. Phys. Chem.* **1993**, *97*, 12523–12529.
- (10) Carrera, A.; Nielsen, I. B.; Çarabal, P.; Dedonder, C.; Broquier, M.; Juvet, C.; Domcke, W.; Sobolewski, A. L. Biradicalic Excited States of Zwitterionic Phenol-Ammonia Clusters. *J. Chem. Phys.* **2009**, *130*, 024302.
- (11) Sobolewski, A. L.; Domcke, W.; Dedonder-Lardeux, C.; Juvet, C. Excited-State Hydrogen Detachment and Hydrogen Transfer Driven by Repulsive $1\pi\sigma^*$ States: A New Paradigm for Nonradiative Decay in Aromatic Biomolecules. *Phys. Chem. Chem. Phys.* **2002**, *4*, 1093–1100.
- (12) Pino, G. A.; Dedonder-Lardeux, C.; Grégoire, G.; Juvet, C.; Martrenchard, S.; Solgadi, D. Intracuster Hydrogen Transfer Followed by Dissociation in the Phenol-(NH₃)₃ excited State: PhOH(S₁)-(NH₃)₃→PhO.⁺(NH₄)(NH₃)₂. *J. Chem. Phys.* **1999**, *111*, 10747–10749.
- (13) Pino, G.; Grégoire, G.; Dedonder-Lardeux, C.; Juvet, C.; Martrenchard, S.; Solgadi, D. A Forgotten Channel in the Excited State Dynamics of Phenol-(Ammonia)(n) Clusters: Hydrogen Transfer. *Phys. Chem. Chem. Phys.* **2000**, *2*, 893–900.
- (14) Miyazaki, M.; Kawanishi, A.; Nielsen, I.; Alata, I.; Ishiuchi, S. I.; Dedonder, C.; Juvet, C.; Fujii, M. Ground State Proton Transfer in Phenol-(NH₃)_n (n ≤ 11) Clusters

- Studied by Mid-IR Spectroscopy in 3-10 Mm Range. *J. Phys. Chem. A* **2013**, *117*, 1522–1530.
- (15) Schultz, T.; Samoylova, E.; Radloff, W.; Hertel, I. V.; Sobolewski, A. L.; Domcke, W. Efficient Deactivation of a Model Base Pair via Excited-State Hydrogen Transfer. *Science* **2004**, *306*, 1765–1768.
 - (16) Shimizu, T.; Hashimoto, K.; Hada, M.; Miyazaki, M.; Fujii, M. A Theoretical Study on the Size-Dependence of Ground-State Proton Transfer in Phenol-Ammonia Clusters. *Phys. Chem. Chem. Phys.* **2018**, *20*, 3265–3276.
 - (17) Kusaka, R.; Nihonyanagi, S.; Tahara, T. The Photochemical Reaction of Phenol Becomes Ultrafast at the Air–Water Interface. *Nat. Chem.* **2021**, *13*, 306–311.
 - (18) Tachikawa, H. Intramolecular Reactions in Ionized Ammonia Clusters: A Direct Ab Initio Molecular Dynamics Study. *J. Phys. Chem. A* **2020**, *124*, 1903–1910.
 - (19) Sadhukhan, D.; Hazra, A.; Naresh Patwari, G. Bend-to-Break: Curvilinear Proton Transfer in Phenol-Ammonia Clusters. *J Phys Chem A* **2020**, *124*, 3101–3108.
 - (20) Sadhukhan, D.; Hsu, P.-J.; Kuo, J.-L.; Patwari, G. N. Is Dissociation of HCl in DMSO Clusters Bistable? *J. Phys. Chem. A* **2021**, *125*, 10351–10358.
 - (21) Neese, F. Software Update: The ORCA Program System, Version 4.0. *Wiley Interdiscip. Rev. Comput. Mol. Sci.* **2018**, *8*, e1327.
 - (22) Boda, M.; Naresh Patwari, G. Insights into Acid Dissociation of HCl and HBr with Internal Electric Fields. *Phys. Chem. Chem. Phys.* **2017**, *19*, 7461–7464.
 - (23) Sen, S.; Boda, M.; Venkat Lata, S.; Naresh Patwari, G. Internal Electric Fields in Small Water Clusters [(H₂O)_n; n = 2–6]. *Phys. Chem. Chem. Phys.* **2016**, *18*, 16730–16737.
 - (24) Fried, S. D.; Boxer, S. G. Measuring Electric Fields and Noncovalent Interactions Using the Vibrational Stark Effect. *Acc. Chem. Res.* **2015**, *48*, 998–1006.
 - (25) Saggu, M.; Levinson, N. M.; Boxer, S. G. Experimental Quantification of Electrostatics in X-H... ϕ Hydrogen Bonds. *J. Am. Chem. Soc.* **2012**, *134*, 18986–18997.
 - (26) Saggu, M.; Levinson, N. M.; Boxer, S. G. Direct Measurements of Electric Fields in Weak OH... π Hydrogen Bonds. *J. Am. Chem. Soc.* **2011**, *133*, 17414–17419.
 - (27) Kühne, T. D.; Iannuzzi, M.; Del Ben, M.; Rybkin, V. V.; Seewald, P.; Stein, F.; Laino, T.; Khaliullin, R. Z.; Schütt, O.; Schiffmann, F.; Golze, D.; Wilhelm, J.; Chulkov, S.; Bani-Hashemian, M. H.; Weber, V.; Borštnik, U.; Taillefumier, M.; Jakobovits, A. S.; Lazzaro, A.; Pabst, H.; Müller, T.; Schade, R.; Guidon, M.; Andermatt, S.; Holmberg, N.; Schenter, G. K.; Hehn, A.; Bussy, A.; Belleflamme, F.; Tabacchi, G.; Glöß, A.; Lass, M.; Bethune, I.; Mundy, C. J.; Plessl, C.; Watkins, M.; VandeVondele, J.; Krack, M.; Hutter, J. CP2K: An Electronic Structure and Molecular Dynamics Software Package - Quickstep: Efficient and Accurate Electronic Structure Calculations. *J. Chem. Phys.* **2020**, *152*, 194103.
 - (28) Mangiatordi, G. F.; Brémond, E.; Adamo, C. DFT and Proton Transfer Reactions: A Benchmark Study on Structure and Kinetics. *J. Chem. Theory Comput.* **2012**, *8*, 3082–3088.
 - (29) Perdew, J. P.; Ernzerhof, M.; Burke, K. Rationale for Mixing Exact Exchange with Density Functional Approximations. *J. Chem. Phys.* **1996**, *105*, 9982–9985.
 - (30) Jin Yong Lee; Sang Joo Lee; Hyuk Soon Choi; Seung Joo Cho; Kwang Soo Kim; Tae-Kyu Ha. Ab Initio Study of the Complexation of Benzene with Ammonium Cations. *Chem. Phys. Lett.* **1995**, *232*, 67–71.